Optimization of platinum dispersion in Pt–PEM electrodes: application to the electrooxidation of ethanol

F. DELIME, J. M. LÉGER, C. LAMY

Laboratoire de Chimie 1, "Electrochimie et Interactions", UMR-CNRS 6503, Université de Poitiers, 40, avenue du Recteur Pineau-86022 Poitiers Cedex, France

---

Nafion$^{®}$ can be used as a solid polymer electrolyte in a PEM fuel cell. Direct platinization of the membrane was realized by chemical reduction of a platinum compound. The platinization procedure was modified to enhance the roughness factor and thus to improve the electrocatalytic activity towards ethanol electrooxidation. The Pt–PEM electrodes were characterized by TEM, atomic absorption analysis, cyclic voltammetry and their polarization curves for ethanol electrooxidation.

Keywords: *Nafion$^{®}$, platinum dispersion, plating conditions, ethanol electrooxidation*

1. Introduction

The electrooxidation of ethanol (C_2H_5OH) is of considerable interest, because of its importance for practical electrocatalytic applications such as in liquid fuel cells, and because it is, with methanol, the simplest compound within the class of aliphatic alcohols [1]. Moreover, as ethanol is a product obtained from renewable sources, it is of special interest for the chemical industry. Recently, ethanol was found to be a promising alternative fuel for direct alcohol fuel cells, with an electrochemical activity comparable to that of methanol [2]. The study of ethanol electrooxidation is, therefore, particularly interesting.

However, the direct electrochemical oxidation of ethanol is not easy, even on platinum, which is the only acceptable catalyst for its oxidation. In fact, surface poisoning of the electrode is always observed, due to the formation of strongly adsorbed species, which are the result of the dissociative adsorption of ethanol. To increase the electrocatalytic activity, the effect of platinum dispersion on the electrode poisoning in the course of ethanol electrooxidation on Pt–PEM electrodes is investigated in this work.

In 1959, Grubb [3] pioneered the use of ionomers as solid polymer electrolytes in batteries, and since that time polymer electrolyte technology has attracted considerable attention. Nafion$^{®}$, which is a copolymer of tetra-fluoroethylene and sulfonyl fluoride vinyl ether, has been widely used as a proton exchange membrane (PEM), because of its advantageous features: namely high protonic conductivity, excellent permselectivity, outstanding chemical and thermal stability, and good mechanical strength. The mainly PEM applications are hydrogen fuel cells [4], methanol fuel cells [4], water electrolysis [5], electro-organic synthesis [6].

For its use as a solid electrolyte in an experimental PEM fuel cell, Nafion$^{®}$ can be metallized, so that the electrocatalytic performances of the composite electrode thus obtained are directly related to the metallic platinum distribution across the membrane thickness [7]. In the literature several methods have been reported for deposition of the platinum catalyst [8]. In this work the impregnation–reduction procedure of platinum deposition was modified [7, 9–11] to improve the metal dispersion, in order to enhance its electrochemical activity for ethanol electrooxidation without increasing the platinum loading. The Pt–PEM electrodes thus obtained were characterized by transmission electron microscopy (TEM), atomic absorption analysis, hydrogen and CO adsorption using cyclic voltammetry, and their polarization curves for ethanol electrooxidation.

2. Experimental details

Perfluorosulfonic acid polymer membranes (Dupont de Nemours, Nafion$^{®}$) were used as the solid polymer electrolyte. Nafion$^{®}$-117 (equivalent weight 1100 and dry thickness 0.178 mm) was chosen because of its commercial availability. Before metal deposition, a three-step standard cleaning procedure was followed for every sample [9]: immersion for 30 min in a boiling $HNO_3 - H_2O$ (1 : 1 by vol.) solution, to remove impurities; immersion for 1 h in boiling milli-Q water (Millipore; resistivity $= 18\,M\Omega\,cm$ at $25\,°C$), to introduce a reproducible amount of water into each sample; then, immersion for 1 h in boiling H_2SO_4 0.5 M $[Pt(NH_3)_4](OH)_2$ (Johnson Matthey) was used as the precursor compound for metallic Pt deposition. $NaBH_4$ from Merck was used as a reducing agent.

The chemical technique to platinize the surface of the Nafion$^{®}$ proton exchange membrane, to form a Pt

electrode, was the impregnation–reduction method according to Millet *et al.* [10] and Fedkiw *et al.* [9]: a given amount of $[Pt(NH_3)_4](OH)_2$ was dissolved in water, and the Nafion® membrane (H^+ form) was soaked for 40 min in this $[Pt(NH_3)_4](OH)_2$ aqueous solution to replace hydrogen ions by platinum ions $[Pt(NH_3)_4]^{2+}$. A given amount of $NaBH_4$ was dissolved in a $LiOH/H_2O$ solution (necessary amount of LiOH to adjust the pH 13) [10–12]. After the impregnation step, the platinum solution was removed from the plating cell and replaced by $40\,cm^3$ of the reducing solution. During both the impregnation and reduction steps, the solution was stirred. The membrane-stirrer distance (2.5 cm) was strictly controlled during each experiment. After the reduction step (2 h), the Pt–PEM composite was soaked in a $0.5\,M\,H_2SO_4$ boiling solution for 2 h, followed by boiling in pure water for 1 h, and then in ultrapure water before use.

Determination of the active surface area of the Pt–PEM electrodes was carried out by the following procedure:

(i) Determination of the quantity of electricity of the hydrogen adsorption region in the cyclic voltammogram after subtracting the double layer charge (a theoretical charge for hydrogen adsorption $Q_H^o = 210\,\mu C\,cm^{-2}$ Pt was used).

(ii) Evaluation of the quantity of electricity associated with the oxidation of CO previously adsorbed. This procedure consists in adsorbing CO at a given potential (+200 mV vs RHE) for a sufficient time (usually 5 min) to obtain a monolayer of CO_{ads}. The Pt–PEM electrode was then purged by nitrogen, with the electrode potential maintained at 200 mV vs RHE. Then, the potential was linearly swept ($v = 20\,mV\,s^{-1}$) to 1.5 V vs RHE to oxidize the preadsorbed CO layer. It was important to check that no oxidation peak appeared during the second sweep, to ensure that the whole CO monolayer was oxidized during the first sweep. The determination of the quantity of electricity for the CO oxidation peak. ($CO_{ads} + H_2O \rightarrow CO_2 + 2H^+ + 2e^-$; $Q_{CO}^o = 420\,\mu C\,cm^{-2}$ Pt) allowed estimation of the active surface area of the Pt–PEM electrode.

For the atomic absorption analysis, in order to determine the platinum loading of the Pt–PEM electrode, the Pt–PEM electrodes were soaked in a $2/3\,HCl + 1/3\,HNO_3$ solution to dissolve platinum. After 12 h, all the platinum was dissolved. Atomic absorption analysis was then performed (Perkin Elmer 3300).

TEM analysis, to examine the surface morphology of the deposit (metal deposit thickness, depth of metal penetration into the Nafion®, distribution of metal particle size) was realized with a Jeol-100 CX or a Philips-CM 120 electron microscope.

To evaluate the poisoning of a Pt–PEM electrode during ethanol electrooxidation, current densities were recorded as a function of time under steady conditions (at $E = 0.4\,V$ vs RHE). For the active
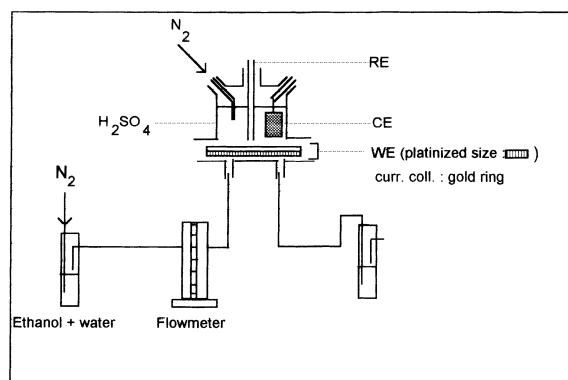

Fig. 1. Scheme of the cell used for voltammetric measurements.

surface area measurements and for the evaluation of electrocatalytic activity, the Pt–PEM electrode was placed in a cell shown in Fig. 1. A $0.5\,cm^2$ disc of the membrane was exposed to a $0.5\,M\,H_2SO_4$ solution on the nonmetallized side and to H_2O (g) or (EtOH/H_2O) (g) on the platinized side. The current collector was a gold ring. The reference electrode was placed directly against the Nafion® membrane on the nonmetallized side. A carbon counter electrode and a reversible hydrogen reference electrode (RHE) were used. Electrolyte solutions were prepared with Millipore Milli-Q water and Merck 'suprapur' chemicals. Cyclic voltammograms were obtained using a Wenking LT-87 potentiostat, a Wenking MVS-87 waveform generator and a Linseis LY-1700 X–Y recorder.

3. Results and discussion

3.1. *Plating procedure to obtain high Pt surface areas: use of the Hadamard matrix*

The application of an iterative method, based on the utilization of the Hadamard matrix [13], was used to evaluate the influence of the experimental conditions on the deposition procedure in order to obtain high Pt surface areas. The interest of such a method results in the limited number of experiments to be carried out, in comparison with the traditional method, for which the effect of individual parameters is successively evaluated, all the other parameters remaining constant during the study. For this iterative method, six successive steps are necessary:

(a) *Choice of the optimization criterion.* In the present case the roughness factor, ρ, of the Pt–PEM electrode is the criterion (ρ = active surface area/geometric surface area).

(b) *Choice of the optimization parameters and determination of the range of variation of these parameters.* In the present work, the platinization procedure was optimized according to four parameters: concentration of the platinum salt ($[Pt(NH_3)_4](OH)_2$), concentration of the reducing agent ($NaBH_4$), temperature and stirring conditions. The choice of the limiting values for each of the previous factors (see Table 1) is the result of preliminary experiments and a literature

Table 1. Limiting values for each of the four studied parameters

Variable	Parameter	−1	+1
U1	Platinum salt concentration	10^{-3} M	10^{-2} M
U2	Reducing agent concentration	2.5×10^{-3} M	10^{-2} M
U3	Temperature during impregnation and reduction	20 °C	50 °C
U4	Stirring speed	30 rpm	230 rpm

search. This takes into account that a good Pt–PEM electrode must have a good contact between each particle, a porous structure to decrease the transport phenomena of reactants to the catalytic sites, a high Pt surface area to enhance the electrochemical activity, and a metal deposit located at, or just beneath, the surface of the membrane, to be accessible for the reactant [9, 12, 14, 15].

(c) *Choice of a mathematical model or a matrix.* In the present work, the Hadamard matrix was chosen [13].

(d) *Determination of the schedule of experiments.* See Table 2.

(e) *Realization of the experiments and estimation of the influence of each factor by calculating coefficients for the determination of the optimization conditions.* Table 3 shows the experimental roughness factors obtained for each of the eight Pt–PEM electrodes prepared. The relative influence of each factor on the chemical deposition process of platinum can be calculated according to [13]:

$$b_x = \frac{1}{2} \left[\frac{\sum_{i=1}^{i=n} \rho_i(+1)}{n} - \frac{\sum_{i=1}^{i=n} \rho_i(-1)}{n} \right]$$

where $\rho_i(\pm 1)$ is the roughness factor of electrode i (level ± 1), n is the number of experiments at level ± 1 and b_x is the estimation coefficient of the studied factor.

Table 4 shows estimation coefficients, b_x, calculated for each studied factor. As can be seen,

the roughness factor clearly depends on the platinum salt concentration, the reducing agent concentration, temperature and stirring conditions. This agrees with [9]. Moreover, the significant influence of the stirring speed is demonstrated, reflected by the high value of b_4. This high sensitivity to stirring conditions may be the result of the modification of the diffusion layer thickness [9]. The stirring speed influences the reducing agent surface concentration. An enhancement of this surface concentration, when decreasing the stirring speed, induces a higher diffusion of the reducing agent into the membrane. This leads to a metal deposit located deeper into the Nafion® membrane. Conversely, an increase in the stirring speed leads to metal deposit located at the membrane surface.

Finally, the optimum parameter values needed to enhance the roughness factor are 10^{-3} M for the platinum salt concentration, 10^{-2} M for the reducing agent concentration, 50 °C for the temperature and 230 rpm for the stirring speed. The concentration values are in good agreement with previously reported work [7].

(f) *Validation of the model by preparing a Pt–PEM electrode under the previous optimum conditions (electrode γ).* For this additional Pt–PEM electrode, the active surface area and the roughness factor estimations were made according to the two methods previously described: determination (i) of the quantity of electricity of the 'hydrogen region' in the cyclic voltammogram or (ii) of that of the oxidation peak associated with the CO monolayer previously adsorbed (Fig. 2). The two methods give a similar value of the roughness factor for the Pt–PEM electrode prepared with the optimum parameter values, 690 and 640, respectively. The shape of the voltammogram is typical of a Pt–Nafion® electrode, and is due to the dispersion of the platinum particles in the Nafion®. So, using these platinization conditions, it is now possible to obtain, with a good reproducibility, roughness factors greater than 600, which is particularly interesting for enhancement of Pt–PEM activity towards the electrooxidation of ethanol.

Table 2. Experiments carried out according to the Hadamard matrix

Experiment	U1 Platinum salt concentration /M	U2 Reducing agent concentration /M	U3 Temperature /°C	U4 Stirring speed /rpm
1	10^{-2}	1.0×10^{-2}	50	30
2	10^{-3}	1.0×10^{-2}	50	230
3	10^{-3}	2.5×10^{-3}	50	230
4	10^{-2}	2.5×10^{-3}	20	230
5	10^{-3}	1.0×10^{-2}	20	30
6	10^{-2}	2.5×10^{-3}	50	30
7	10^{-2}	1.0×10^{-2}	20	230
8	10^{-3}	2.5×10^{-3}	20	30

Table 3. Active surface area and roughness factor of the eight studied Pt–PEM electrodes

Experiment	1	2	3	4	5	6	7	8
Active surface area/cm^2	50	320	117	180	32	23	44	27
ρ		100	640	234	360	64	46	88	54

Table 4. Estimation coefficients b_x calculated for each studied factor

Platinum salt concentration	$b_1 = -62$
Reducing agent concentration	$b_2 = +37$
Temperature	$b_3 = +69$
Stirring speed	$b_4 = +120$

However, the atomic absorption analysis indicates that the platinum loading related to the geometric surface area (mg cm^{-2}) is similar (~ 1.2 mg cm^{-2}), whatever the deposition conditions, for the studied parameter range (Table 5). This indicates that these deposition conditions only influence the platinum dispersion by enhancing the surface deposit thickness and, therefore, by decreasing the quantity of platinum located too deeply into the Nafion®, so that it is still accessible by any reacting molecule.

3.2. Evaluation of Pt–PEM electrodes by TEM examination

Figure 3 shows TEM photographs of Pt–PEM electrodes, the active surface area and roughness factor of which are summarized in Table 6. We made the assumption that the Pt-particles located into the Nafion® underneath the surface deposit have sizes comparable to those constituting the metal surface deposit. The comparison of TEM observations for these Pt–PEM electrodes allows visualization of the influence of the Pt deposition parameters on the real surface morphology of the deposit at submicrometric scale: metal-deposit thickness, depth of metal penetration into the membrane, size distribution of metal particles.

These TEM observations suggest that the deposition method has a strong influence on the electrode active surface area because of the metal deposit thickness. In fact, there is a strong dependancy of the deposit thickness on the real surface area of the electrode. As an example, the Pt particle sizes are comparable for the electrodes δ and ε, however, the metal deposit thickness for the Pt–PEM electrode δ is 2.5 times greater than that for the Pt–PEM electrode ε. Consequently, the active surface area for the Pt–PEM electrode δ is 1.5 larger than that for the Pt–PEM electrode ε.

3.3. Modelling of experimental results

3.3.1. Description of the model. The specific surface area is a macroscopic parameter, useful in the characterization of dispersed catalysts, but not for visualising the corresponding surface morphology. By using a simple structural model, and by fitting it to the active surface area, assumptions concerning the surface morphology may, however, be derived and compared to the structural characterization (by TEM) of the electrode surfaces.

In the following simple model the deposit was considered as homogeneously distributed spherical particles. The characteristic particle diameter, d (nm), was then related to the specific surface area, S (m^2 g^{-1}), by

$$d = \frac{6000}{S\mu} \tag{1}$$

with S given by
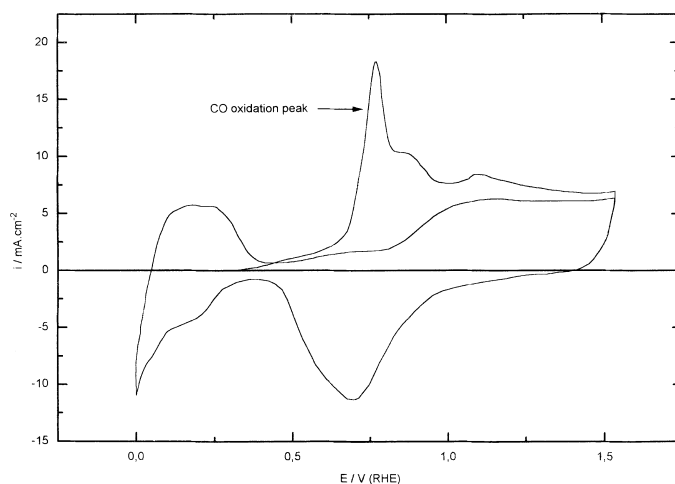
$$S = \frac{1000 A_r}{A_g W} \tag{2}$$

Fig. 2. Cyclic voltammograms of a Pt–PEM electrode (electrode γ) allowing to determine the real surface area by (i) integration of the $i(E)$ curve in the 'hydrogen adsorption region' and (ii) integration of the $i(E)$ curve corresponding to the CO oxidation peak (0.5 M H$_2$SO$_4$, $v = 10$ mV s^{-1}; $T = 20\,^\circ$C).

Table 5. Platinum loading (related to the geometric surface area) of two Pt–PEM electrodes prepared under different deposition conditions

Platinum salt concentration	1×10^{-3} M	1×10^{-3} M
Reducing agent concentration	1×10^{-2} M	0.5 M
Temperature	50 °C	20 °C
Stirring speed	230 rpm	30 rpm
Platinum loading	1.24 mg cm^{-2}	1.30 mg cm^{-2}

where $\mu = 21.4$ g cm^{-3} (platinum density), A_r is the Pt active surface area, A_g is the Pt geometric surface area and W the metal loading (μg cm^{-2}).

The calculated Pt active surface area, A_r was then related to the characteristic particle diameter, d (nm), by

$$A_r = \frac{6WA_g}{\mu d} \qquad (3)$$

It is also assumed in this model that most of the Pt particles are accessible, which means that most of the Pt particles are deposited on or near the surface of the Nafion® membrane. This assumption is roughly in agreement with the TEM images.

3.3.2. Comparison of TEM images and model results. Although the TEM images of the electrode γ (characteristics given in Table 6) show that homogeneously distributed spherical Pt particles are not achieved (particles size from 5 to 25 nm), we can determine a value for the average particle size ($\overline{d}$). This was obtained by measuring the diameter of a sufficient number of particles to ensure a good statistical representation. The surface mean diameter, $\overline{d}$, of the Pt particles was calculated from the size distribution, using $\overline{d} = \sum f_i d_i^3 / \sum f_i d_i^2$, where f_i is the frequency of occurrence of the particles of diameter d_i in the sample [19]. We obtained a value of 16 nm for $\overline{d}$. The calculated active surface area for the electrode γ, determined from the model, is then $A_r = 108$ cm^2, that is, for $\rho = 216$. The experimental value ($\rho = 690$), determined by hydrogen adsorption–desorption coulometry, is larger by a factor of about 3 than the value obtained from the simple model considered here.

The discrepancy between calculated and experimental ρ values requires explanation. Although the TEM images show that homogeneously distributed spherical Pt particles are not obtained, using this model suggests Pt particles of diameter 5 nm give the

measured roughness factor, that is, $\rho = 680$ for $d = 5$ nm, $A_r = 340$ cm^2, which would be in a very good agreement with the value obtained experimentally. This corresponds to the smallest particles observed in the TEM images. Calculation of the average Pt diameter (16 nm) from TEM gives an underestimation of the roughness factor as the Pt particles are assumed to be smooth in the theoretical model. This suggests that the larger Pt particles agglomerate to generate their own microroughness: if the largest Pt particles ($d \approx 25$ nm) have a microstructure, that is, a roughness factor of about 5 for the particle itself, the model gives the same active surface area as the electrochemical evaluation. This microporosity is also observed in the TEM image (Fig. 3, TEM Image A). Wavy surface structures have already been observed [20] by STM in the case of Pt microparticles deposited *electrochemically* on glassy carbon, because of nucleation sites. In the present work, the Pt particles were deposited *chemically* on Nafion®. Such a fine structure for chemically deposited particles is probably due to the long reduction time.

These deposition conditions, therefore, allow optimization of the platinum surface accessible to the reacting molecules because of the microroughness of the platinum particles.

3.4. *Influence of the Pt-dispersion on the Pt–PEM electrode activity on ethanol electrooxidation*

The electrochemical oxidation of ethanol on platinum leads to surface poisoning of the electrode due to the formation of strongly adsorbed species resulting from dissociative adsorption. In the case of ethanol electrooxidation in acid medium, the electrode surface coverage by strongly adsorbed species, particularly CO_{ads} species, is very high [16]. The crystallite size of dispersed noble metal electrodes, as expected from particle size effects in heterogeneous catalysis, plays a definite role in the chemisorption step [17, 18]. This suggests that the rate of poisoning for dispersed electrodes is much lower than for smooth electrodes under similar experimental conditions. There is a clear difference in the behaviour of dispersed platinum as compared to that of smooth platinum in the case of the chemisorption and electrooxidation of ethanol.

Figure 4 shows the effect of the platinum dispersion on Nafion®-117 on the electrochemical activity of a Pt–PEM electrode. It is clear that the current

Table 6. Macroscopic and submicroscopic (TEM) characteristics (Pt particle size and metal deposit thickness) of the observed Pt–PEM electrodes

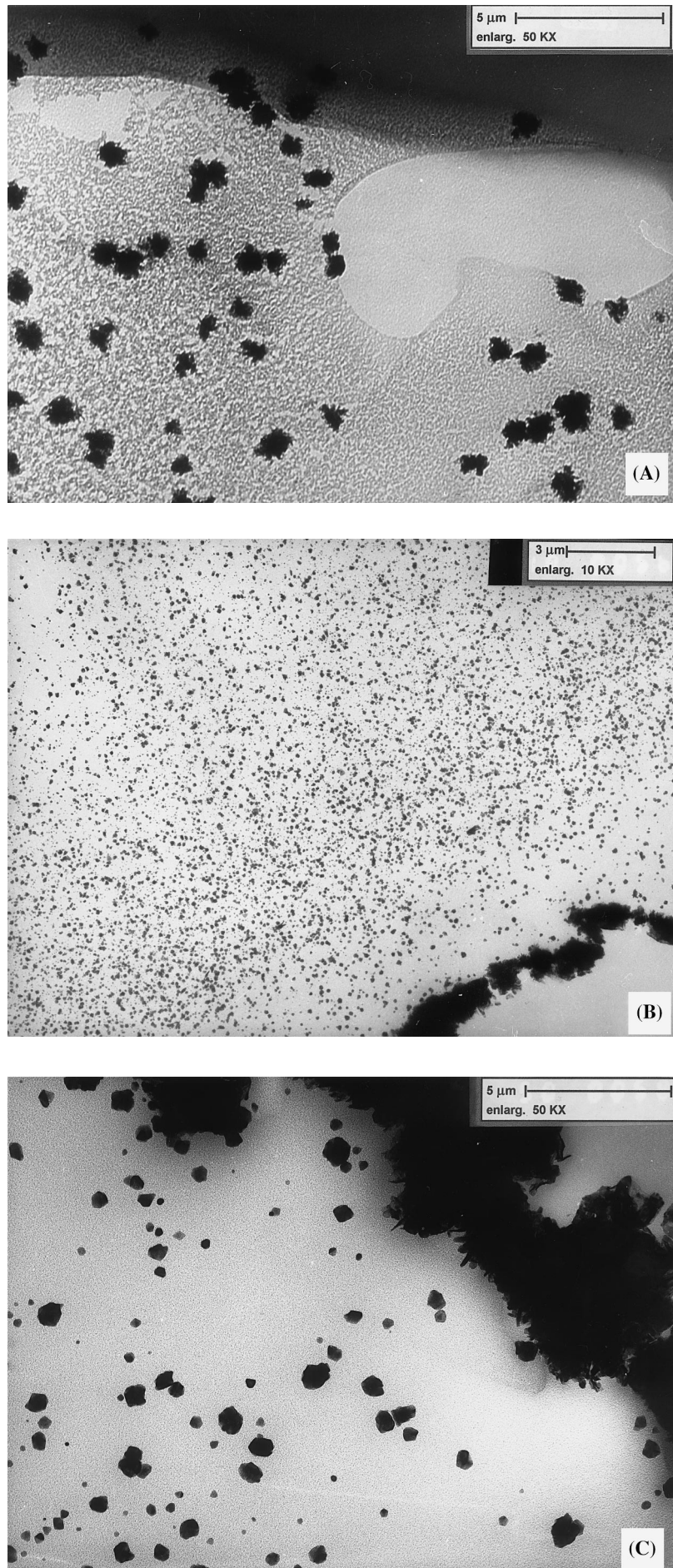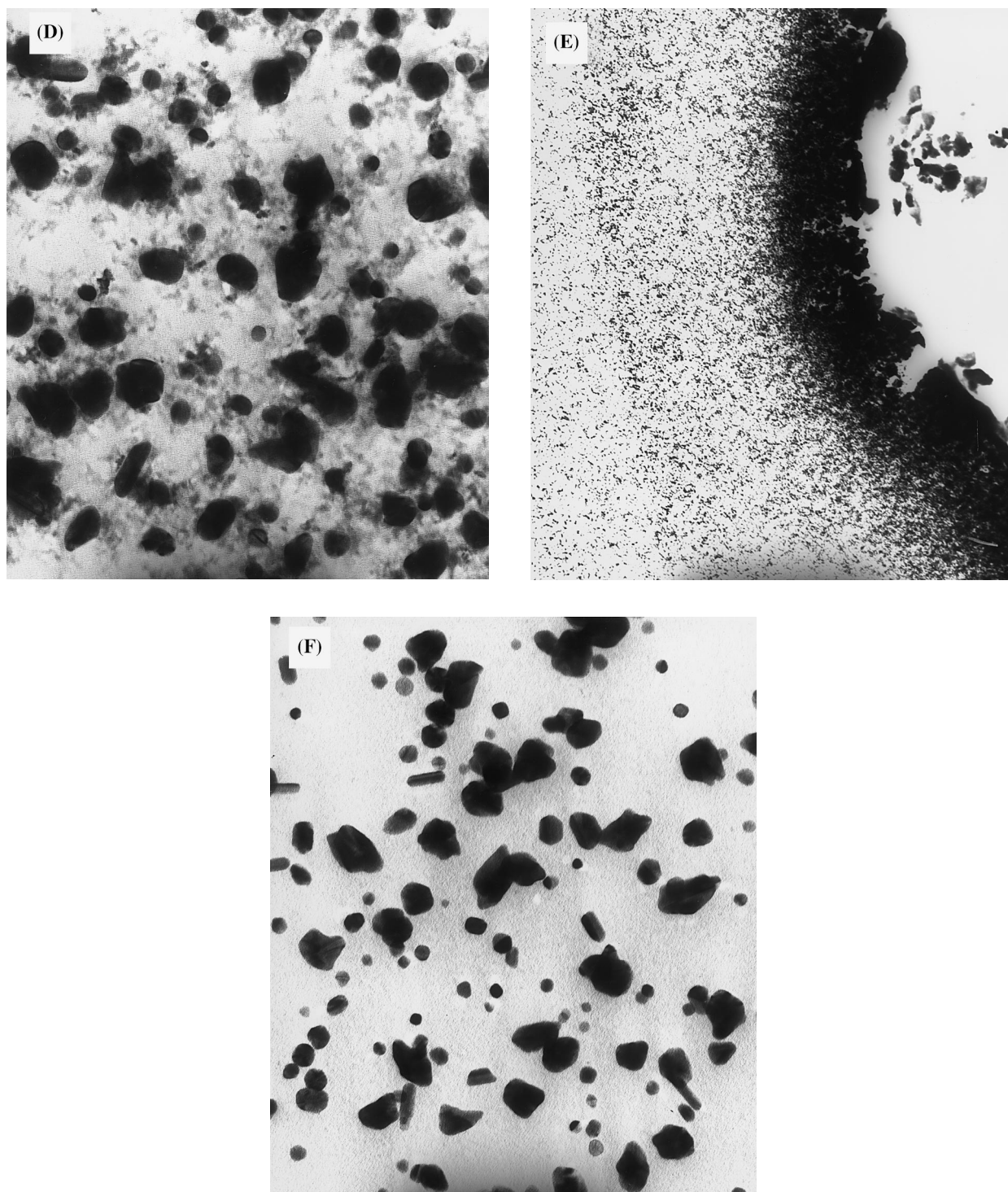| Electrode	Active surface area /cm^2	Roughness factor	Pt particle size /nm	Metal deposit thickness /μm
β	2	4	60	–
ε	90	180	15 to 50	0.4
δ	140	280	10 to 40	1.0
γ	345	690	5 to 25	2.0

Fig. 3. A–C

Fig. 3. TEM photographs of several Pt–PEM electrodes. (A) ($\times$ 22 500): electrode β; (B) ($\times$ 4500), (C) ($\times$ 22 500): electrode ε; (D) ($\times$ 90 000), (E) ($\times$ 3600): electrode δ; (F) ($\times$ 90 000): electrode γ.

density related to the active surface area (at a constant value of potential) increases with platinum dispersion by shifting the Tafel plot cathodically: for example at 500 mV vs RHE, the current density is enhanced by a factor of 3. However, the same value of the Tafel slopes shows that there is no change in the reaction mechanism, particularly the rate determining step. This suggests a weaker poisoning for highly dispersed Pt–PEM electrodes.

The influence of the Pt dispersion on the poisoning phenomena of two Pt–PEM electrodes during ethanol electrooxidation is illustrated in Fig. 5. The decrease of i with time shows the occurrence of poisoning for the two Pt–PEM electrodes, whatever the roughness factor value. On the other hand, as shown in the $\mathrm{d}i/\mathrm{d}t$ against t plots (Fig. 6), from $t = 0$ to $t = 2\,\mathrm{min}$, it clearly appears that an increase in the Pt active surface area leads to a lower poisoning rate, according to the smaller value of the slope when $\rho = 320$ in comparison with that for $\rho = 20$ (slopes 0.25 and 0.4, respectively).
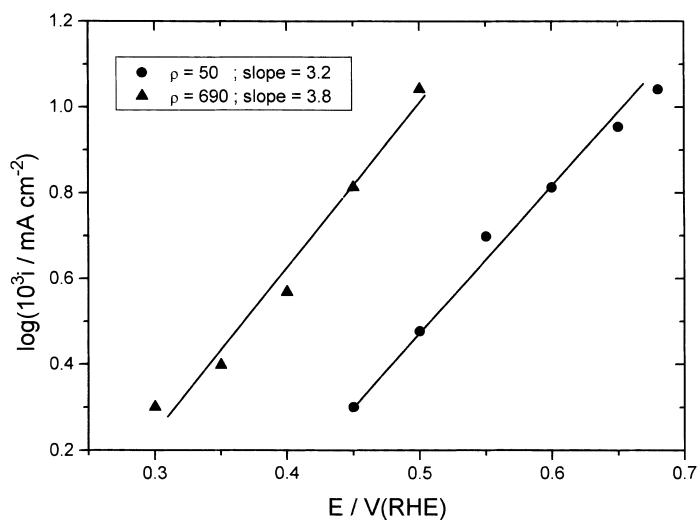
Fig. 4. Influence of the platinum dispersion on the activity of a Pt–PEM electrode for ethanol electrooxidation: comparison of the Tafel plots of two Pt–PEM electrodes with different roughness factors (i related to the active surface area; EtOH = 10% in volume; flow rate $35\,cm^3\,min^{-1}$; $v = 10\,mV\,s^{-1}$; $T = 20\,^{\circ}C$).
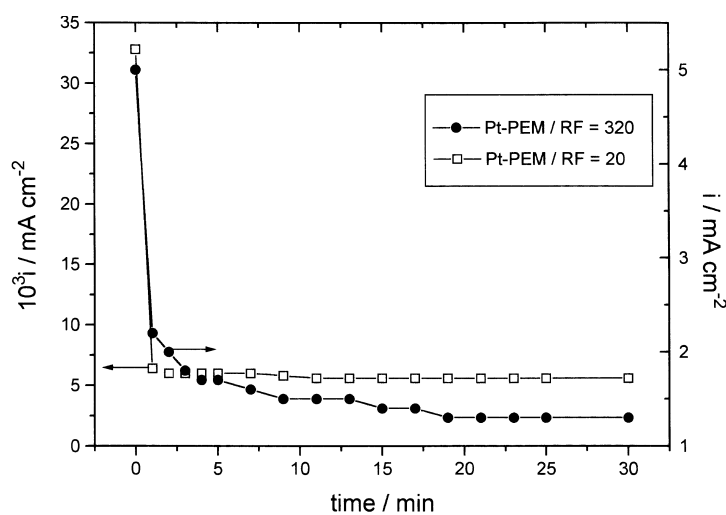
Fig. 5. Comparison of the poisoning rate of two Pt–PEM electrodes with different roughness factors (i related to geometric surface area; $E = 0.4\,V$ vs RHE; EtOH = 10% in volume ; flow rate $35\,cm^3\,min^{-1}$; $v = 10\,mV\,s^{-1}$; $T = 20\,^{\circ}C$).
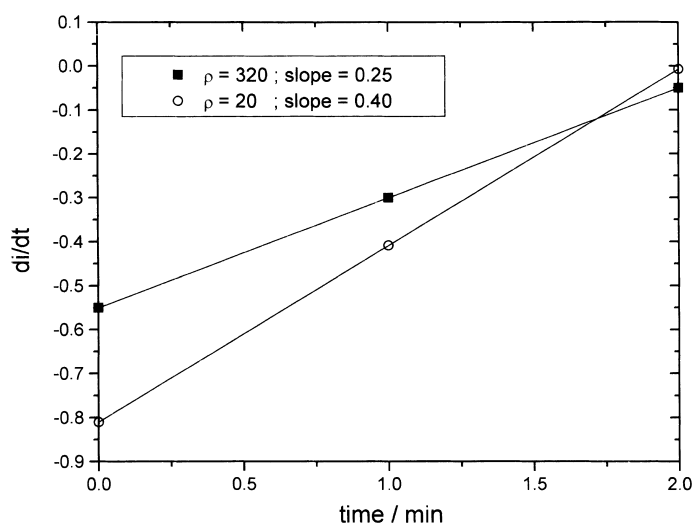

Fig. 6. di/dt (normalized scale) against t plots from $t = 0$ to $t = 2\,min$ for two Pt–PEM electrodes with different roughness factors.

4. Conclusion

The application of an iterative method (the Hadamard matrix) is particularly interesting for the determination of the influence of several platinization parameters on the roughness factor of Pt–PEM electrodes prepared by the impregnation–reduction plating procedure. The optimum parameter values needed to enhance the roughness factor of a Pt–PEM electrode are 10^{-3} M for the platinum salt concentration, 10^{-2} M for the reducing agent concentration, $50\,^{\circ}\text{C}$ and 230 rpm for the stirring speed. With these platinization conditions it is possible to obtain, with good reproducibility, roughness factors greater than 600 by increasing the metal deposit thickness and decreasing the quantity of platinum located too deeply into the Nafion®, so that it becomes inaccessible to the reactant molecules. The use of such a Pt–PEM electrode for ethanol electrooxidation leads to enhanced oxidation current densities and shifts the oxidation peaks towards more cathodic potentials. Moreover, electrode poisoning during ethanol electrooxidation decreases when the roughness factor of the Pt–PEM electrode is increased. Similar results were obtained for methanol electrooxidation [21].

Acknowledgements

References

[1]   R. A. Rightmire, R. L. Rowland, D. L. Boos and D. L. Beals, *J. Electrochem. Soc.* **111** (1964) 242.
[2]   J. Wang, S. Wasmus and R. Savinell, *ibid.* **142** (1995) 4218.
[3]   W. T. Grubb, *J. Electroanal. Chem.* **106** (1959) 275.
[4]   K. Kordesch and G. Simader *in* 'Fuel Cells and their Applications', VCH, Weinheim (1996), p. 151.
[5]   G. C. Scherer, T. Momose and K. Tomiie, *J. Electrochem. Soc.* **135** (1988) 3071.
[6]   H. Nakajima and H. Kita, *Electrochim. Acta* **33** (1988) 521.
[7]   P. Millet, F. Andolfatto and R. Durand, *J. Appl. Electrochem.* **25** (1995) 233.
[8]   R. Mosdale and S. Srinivasan, *Electrochim. Acta* **40** (1995) 413.
[9]   R. Liu, W. H. Her and P. S. Fedkiw, *J Electrochem. Soc.* **139** (1992) 15.
[10] P. Millet, M. Pineri and R. Durand, *J Appl. Electrochem.* **19** (1989) 162.
[11] P. Millet, F. Andolfatto and R. Durand, *ibid.* **25** (1995) 227.
[12] P. S. Fedkiw and W. H. Her, *J. Electrochem. Soc.* **136** (1989) 899.
[13] G. E. P Box and N. R. Draper, 'Empirical Model Building and Response Surfaces', J. Wiley & Sons, New York (1987); G.E.P Box, W. G. Hunter and J. S. Hunter 'Statistics for Experimenters', J. Wiley & Sons, New York (1978).
[14] E. A. Ticianelli, J. G. Beery and S. Srinivasan, *J. Appl. Electrochem.* **21** (1991) 597.
[15] H. Takenaka, E. Torikai, Y. Kawami and N. Wakabayashi, *Int J. Hydrogen. Energy* **7** (1982) 397.
[16] B. Beden, M. C. Morin, F. Hahn and C. Lamy, *J. Electroanal. Chem.* **229** (1987) 353.
[17] B. Beden, J. M. Léger and C. Lamy *in* 'Modern Aspect of Electrochemistry', Vol. 22 (edited by J. O'M. Bockris, B. E. Conway and R. E. White), Plenum Press, New York (1992), ch. 2, p. 97.
[18] B. Beden, F. Hahn, C. Lamy, J. M. Léger, N. R. de Tacconi, R. O. Lezna and A. J. Arvia, *J. Electroanal. Chem.* **261** (1989) 401.
[19] A. Gamez, D. Richard., P. Gallezot, F. Gloaguen, R. Faure and R. Durand, *Electrochim. Acta* **41** (1996) 307.
[20] K. Shimazu, K. Uosaki, H. Kita and Y. Nodasaka, *J. Electroanal. Chem.* **256** (1988) 481.
[21] B. Beden, C. Lamy, N. R. de Tacconi and A. J. Arvia *Electrochim. Acta* **35** (1990) 691.